An Investigation of the Cooling Properties of a Sapphire Half-Wave Plate for SPIDER

Thesis by

Abigail T. Crites

In Partial Fulfillment of the Requirements

for the Degree of

Bachelor of Science

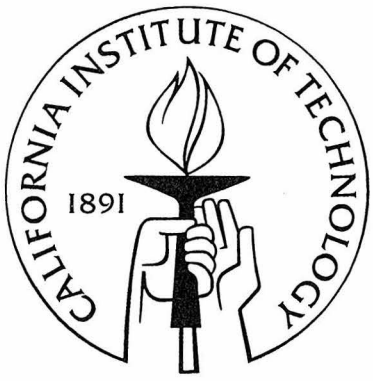

California Institute of Technology

Pasadena, California

2006

(Submitted 1 May, 2006)

Acknowledgements

I would like to thank my senior thesis advisor, Professor Andrew Lange, for his support as well as the SURF office for their financial support during the summer. I would like to thank Bill Jones for teaching me so much about lab work and about this field in general and also for reading and editing this thesis. Thanks go also to Kathy Deniston, the people in the Caltech Machine Shop, Peter Ade and Carole Tucker for providing me with the things I needed to complete this project. I also must thank Barth Netterfield, John Kovac, Brian Keating, Christian Reichardt and the entire observational cosmology group here at Caltech for giving me advice and answering my many questions.

Abstract

Specific cryogenic data about the thermal and optical properties of sapphire are required to properly implement the sapphire half-wave plate that will be used to modulate the polarization signal in the next generation of CMB polarimeters. The wave plate must be operated from a base temperature of between 4 and 20 K. Simulations and experiments in a cryostat will determine if the sapphire sample can be radiatively cooled to approximately 20 K when operating from a 4.2K base temperature. These data will be used to design the final wave plate mount and determine how it will be operated.

Contents

Chapter 1

Introduction

The cosmic microwave background (CMB) has been extensively studied by cosmologists who are interested in understanding the very early universe. The CMB is remnant radiation from the early epoch when the matter and radiation first cooled enough for photons to decouple from matter [1]. This radiation .is described by its spectrum, spatial distribution of intensity, and spatial distribution of polarization [2]. By studying the CMB temperature anisotropies cosmologist have been able to put constraints on cosmological constants and get a better picture of the early universe within the constraints of standard inflation cosmologies. Now cosmologists wish to do further CMB research to directly probe the theory of inflation. This theory hypothesizes that the universe expanded from a very small size rapidly in the early history of the universe. If this theory is correct the rapid expansion would have produced gravitational waves. These gravitational waves would leave an imprint on the CMB in the form of polarization. For this reason, the goal of many current CMB experiments is to measure the polarization of the CMB [3].

SPIDER is an experiment that has been proposed to comprehensively study the polarization of the CMB on large scales. This will be a balloon-borne experiment with six telescopes and the capability to cover 60% of the sky. One of the requirements for this project is a method of polarization modulation. It has been proposed to use a twelve inch diameter sapphire half-wave plate to do the polarization modulation. In this experiment the wave plate will need to be cooled to between 4K and 20K and spun at 10Hz. Because it must be spun so quickly, it will be magnetically levitated using a superconducting bearing [3]. It has been proposed that an ideal method of cooling the plate would be through radiative cooling. This method is ideal for this application because it requires no mechanical contact to the wave plate while in operation. However, a downside to this method is that radiative cooling is very inefficient at the temperature range in which this disk will operate. This paper discusses experiments that lead to a collection of cryogenic data about optical, material, and thermal properties of the sapphire wave plate that will determine how the cooling of the wave plate will be implemented in its application in SPIDER.

Chapter 2

Scientific Context

2.1 The Cosmic Microwave Background

Over the last 30 years the CMB has emerged as an incredibly powerful tool in determining cosmological parameters of the standard model of cosmology. From the time of its discovery until the present scientists have designed and run instruments to probe the CMB. The very discovery of the CMB, helped substantiate the big bang theory of the origin of the universe, and it was soon clear that this phenomenon should be studied and the spectrum of the CMB measured.

SPIDER is the next step in terms of technology and science in a progression of CMB experiments. The earlier CMB experiments mapped the temperature anisotropy and determined the power spectrum. A plot of this can be seen in figure 2.1. This allowed scientists to put constraints on Ω_λ and Ω_m which showed that the universe is flat [4]. This science was done with both bolometric detectors and coherent detectors.

After the temperature power spectrum of the CMB was well characterized, work began on the next generation of experiments. These experiments were built to determine the polarization of the CMB. There are two kinds of polarization that theory predicts. The first is the E-mode or curl free component that results from the density perturbations present during the epoch of recombination. The second is the B-mode or curl component of the polarization which, on large angular scales is generated primarily by primordial gravitational waves. It is important to cosmology to detect the curl free component of the CMB polarization, because the current inflationary models predict the existence of this phenomenon. If this polarization were not found then the current theories would have to be revisited [5], [6].

There are published results that describe detection of the curl free component, but the curl component has yet to be detected. Some of the experiments that detected the E mode polarization were DASI, CBI, WMAP, CAPMAP and Boomerang. DASI and CBI were interferometers that used coherent detectors to measure the polarization[7], [8]. WMAP and CAPMAP also used coherent detectors, but were not interferometers. The Boomerang experiment was the first bolometric

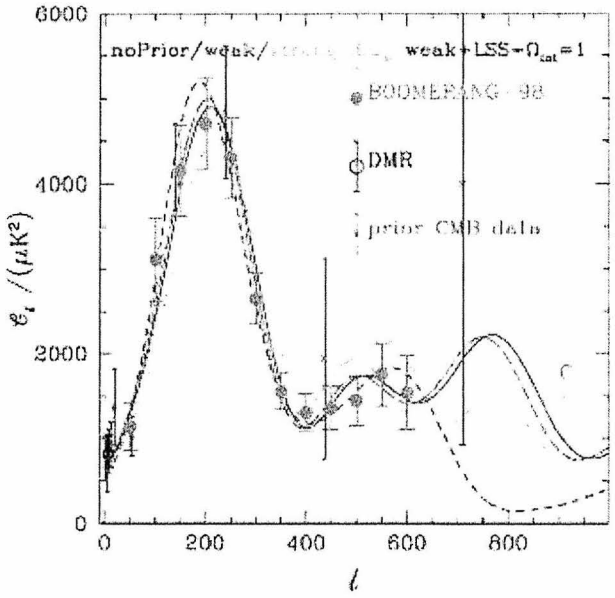

Figure 2.1: from Cosmological Parameters from the first results of Boomerang, as accepted by Phys.Rev.D, A. E. Lange, et. al. This shows the power spectrum of the CMB. The x axis is l, the multipole moment and the y axis is amplitude of the signal.

experiment to detect polarization [9].

The next generation of experiments are designed to detect the B mode polarization. There are currently two in the field, the South Pole based QUAD and Robinson telescopes. These are experiments with bolometric detectors. SPIDER is the logical next step in the progression of CMB polarization technology. The knowledge gained from currently operating experiments such as Robinson will provide invaluable information about the technology that will be used in SPIDER.

2.2 Polarization Modulation: Half-Wave Plate

One of the main obstacles to overcome when designing a highly sensitive instrument to detect CMB polarization is finding an appropriate method of polarization modulation. Some of the methods past and current CMB experiments have used are sky rotation, faraday rotators, a half-wave plate, and micro electro mechanical (MEM) or other switches [10]. When detecting polarization the detector will see the polarized signal = I + Q cos(2θ) + U sin(2θ), where θ is the angle between the detector and the linear polarization of the light. Polarization modulation allows the I, Q and U parameters to be determined from the incident polarized signal. SPIDER will use a half-wave plate for polarization modulation, which works as described in figure 2.2. The half wave plate will be placed in the optical train of each monochromatic telescope on SPIDER as shown in 2.3. A half-wave plate is ideal for

polarization modulation because it can be placed in front of the optics and therefore modulates only the sky and does not modulate any effects from the optics. The other methods of modulation mentioned here do not have that advantage [10].

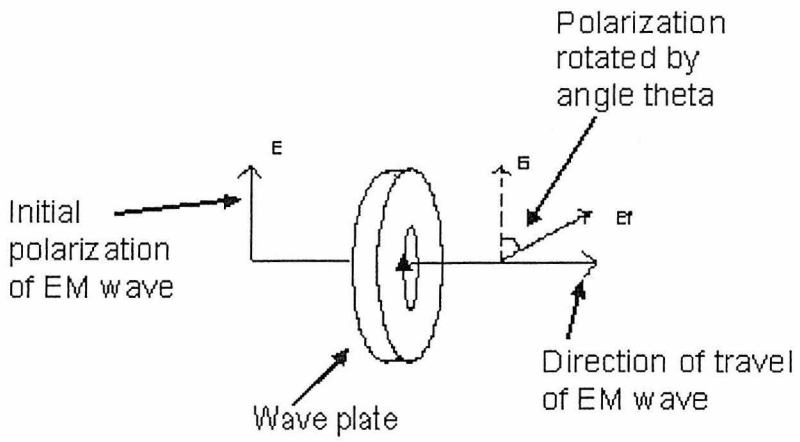

Figure 2.2: Sketch of the polarization modulation of an incident polarized signal by the wave plate.

The frequency at which to spin the half-wave plate is determined by the noise properties of the detectors and the details of the scan strategy. The mechanical and thermal constraints on the wave plate design require that a method of cooling the wave plate is used that does not require physical contact. For this reason radiative cooling was picked as the optimal method of keeping the wave plate at around 20 K. The wave plate must be kept cold so that the radiative background is minimized.

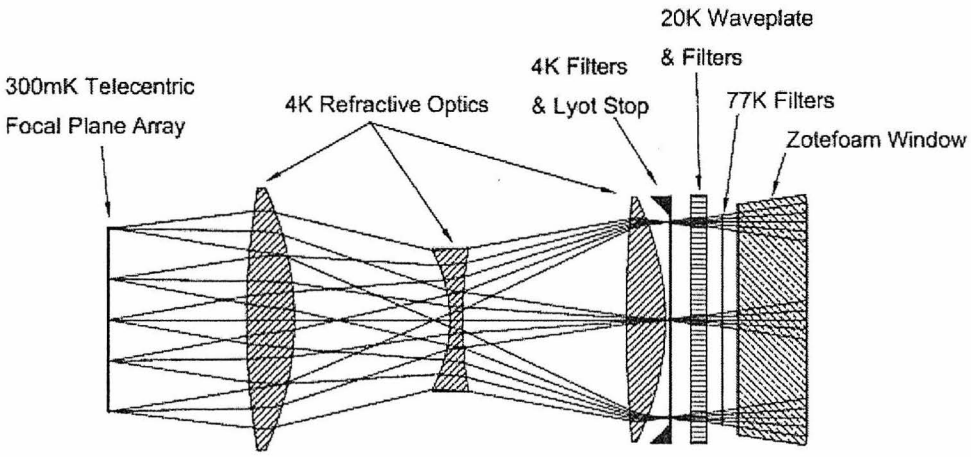

Figure 2.3: The placement of the half-wave plate in the SPIDER optical train

Chapter 3

Experimental Apparatus

3.1 Cryostat Configuration for Dark Tests

The apparatus being used to test the properties of the wave plate is a liquid nitrogen/ liquid helium cryostat. The location of the sample is in a vacuum space surrounded by a radiation shield and coupled to a liquid helium (4.2K) bath. This stage is itself isolated from room temperature by the 77K bath and radiation shield cooled by liquid nitrogen. The sample is suspended off of three aluminum rods using Kevlar thread. This is shown in figure 3.1 and figure 3.2.

Kevlar thread is used to suspend the sample because of its very low thermal conductivity. Shown below are calculations of the thermal conductivity of Kevlar that demonstrate that the Kevlar supports will not significantly contribute to the cooling of the sapphire.

Thermal conductivity of Kevlar at 4K: $3 \cdot 10^{-4} W/cmK$. So for 30K$\rightarrow$ 4K: [11]

$$\begin{aligned} \text{power} &= (3 \cdot 10^{-4}\text{W/cm} \cdot \text{K} \cdot (0.014\text{ in})^2 \cdot \pi \cdot 2.54\text{cm/in} \cdot \Delta X degrees)/1\text{in} \\ &= 1.22 \cdot 10^{-5}\text{W} \\ &= 0.012\text{mW} \end{aligned} \tag{3.1}$$

The devices that are needed for these tests are thermometers on the 4 K shield and on the sapphire sample and a heater on the sample. A simple metal film resistor is used as a heater. For thermometry Silicon diodes from Lake Shore Cryogenics are used. The diodes are calibrated to 0.25K and will have 4 leads. At cryogenic temperatures however, 4 leads are not needed because the resistance of the wire is negligible so only a two lead measurements are done. Below is the calculation showing the voltage contributed from 1m long leads.

Wire resistance: 8.56ohms/m

$$V = IR = 10 * 10^{-6} Amps * 2 * 1m * 8.56 ohms/m = 1.71 * 10^{-4} V \tag{3.2}$$

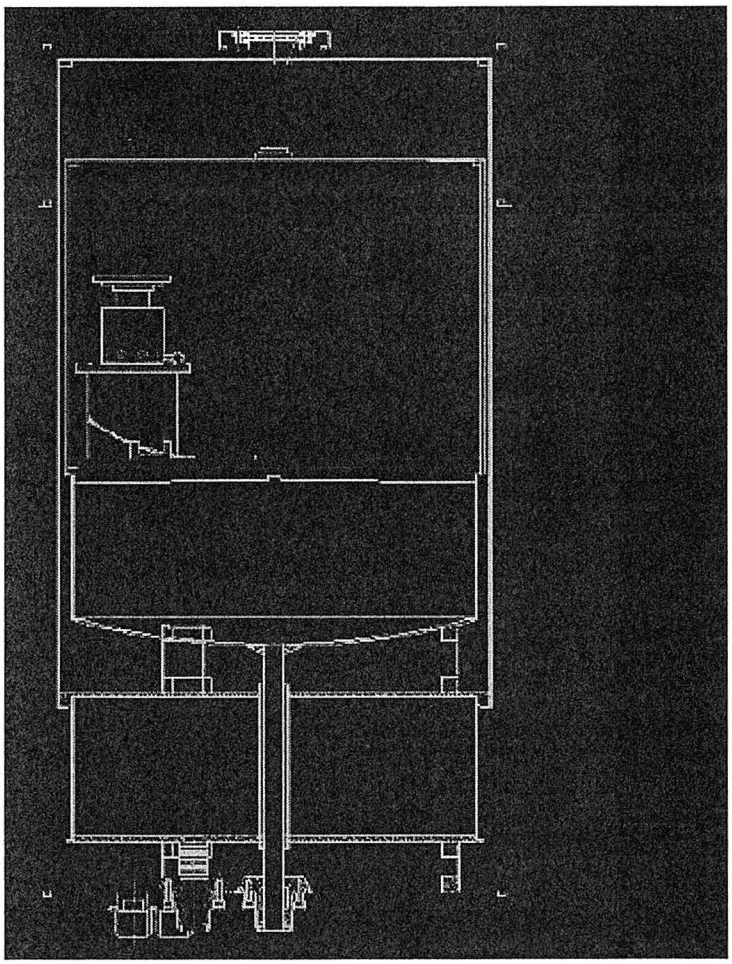

Figure 3.1: AutoCad drawing of the dewar. (courtesy of Bill Jones)

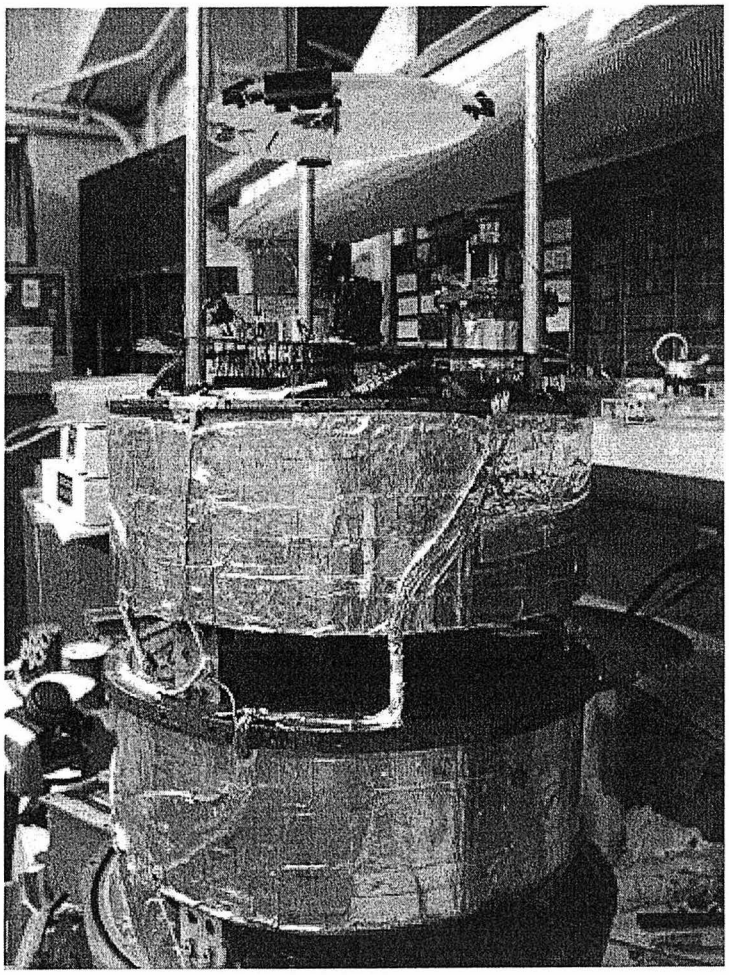

Figure 3.2: Photo of the dewar with sapphire suspended from Kevlar threads

	Location and Number of Diodes	Location and Number of Heaters
Run 1-6	One diode on each of the 4K shield, the base plate, the blackened base plate, and one of the support posts and two diodes on the sample.	One heater on the sample.
Run 7	One diode on each of the 4K shield, the base plate, the blackened base plate, and one of the support posts and three diodes on the sample.	One heater on the warm load.

Table 3.1: Diode and heater location

From the Lake Shore Cryogenics' data sheets we know that dV/dT = -33.6 mV/K at 4.2K, so the excess voltage in the leads corresponds to an excess temperature of 0.005K [12], and is therefore negligible.

As mentioned above it is important to determine the contribution of the wires to the thermal conductivity between the sample and the 4K bath. Thermal conductivity of Phosphor Bronze leads is 10W/m*K at 20K, 4.6W/m*K at 10K and 1.6W/m*K at 4K. For the 36 gauge wire being used in this experiment, the area of the wire is $1.27 * 10^{-8}$ square meters [12]. Using this information the parasitic thermal conductivity provided by the wires can be calculated using the method show in appendix C1 This will be discussed in more detail in the results section as it relates to the specific analysis of the data. The thermometer data is continuously recorded on a local PC.

The location and number of diodes for each run can be found in table 3.1. The diodes were attached to the samples using Apiezon N low temperature conductive grease and clamps or tape as shown in 3.3.

The setup for the second run was similar to the first, except a new 4K shield was constructed from copper and painted with a Stycast epoxy and carbon mixture. This new shield was implemented because copper has a higher thermal conductivity than aluminum and would therefore be more likely to stay at a stable temperature. The Stycast and carbon mixture has a high emissivity and is designed to cause the shield to couple well radiatively to the sample [11]. A thin-walled stainless steel gas-gap heat switch was used to attach the sample to the cold stage.

Eventually, a 6 inch diameter by 0.1 inch thick sapphire plate is tested, but in the first four tests discussed here an aluminum disk of the same size is used for the test. The reason for this is that we wish to get a control measurement to compare the sapphire measurement to. As mentioned above, during the first run the sample was bare aluminum.

For the second, third and fourth runs the aluminum disk was blackened with the carbon and Stycast mixture. The blackened aluminum disk is a good choice for a baseline test because its emissivity is close to one and we wish to discover how different from one the emissivity of sapphire

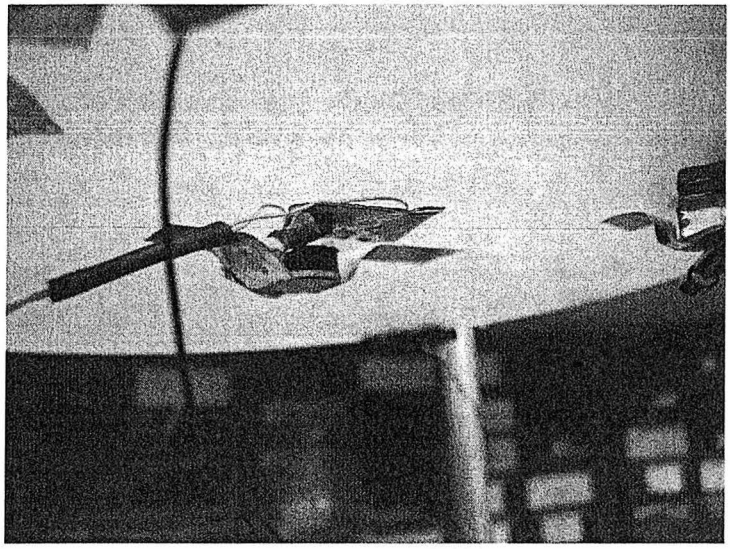

Figure 3.3: A photograph of a diode thermometer taped to the sapphire wave plate

is from one. The sample also has a heater attached to it to apply power to the disk when needed.

The cryostat and shield configuration for the third run was similar to the second, except there was no heat switch attaching the sample to the 4K stage. The configuration for the fourth run was the same as for the third run. For the fifth run the configuration was kept constant, but the blackened aluminum disk was replaced with the actual 6 inch diameter by 0.1 inch thick sapphire sample.

3.2 Modifications for Optical Tests

A final run was done where the configuration was changed to allow the ability to test filters similar to the ones that will be used in SPIDER. This will determine if the filters are sufficient to reduce the optical loading on the sapphire such that it will stay cold in operation.

For this run the four filters where heat sunk to the 4K cooled shield. The filters are designed to block the out of band radiation and prevent that radiation from warming the optics. The transmission of the three thermal filters can be seen in figure 3.4 plotted with the 80K blackbody curve. The transmission of the LPE filter is plotted in figure 3.5 with the 20K blackbody curve [13].

The approximate power that is expected to reach the wave plate through the filters is calculated by integrating the section of the blackbody curve that is in the transmission region of the LPE filter. This transmitted power as a function of optical load temperature can be seen in figure 3.6.

A temperature controlled warm load was placed in front of the thermal filters. This load is thermally coupled to the 4K bath through a tin heat switch, and controlled with a silicon diode thermometer and a metal film resistive heater. The thermal properties of tin are optimal for this

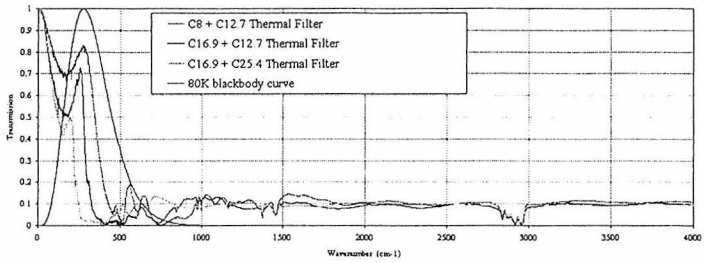

Figure 3.4: The filter transmission for the thermal filters plotted with a normalized 80K blackbody curve

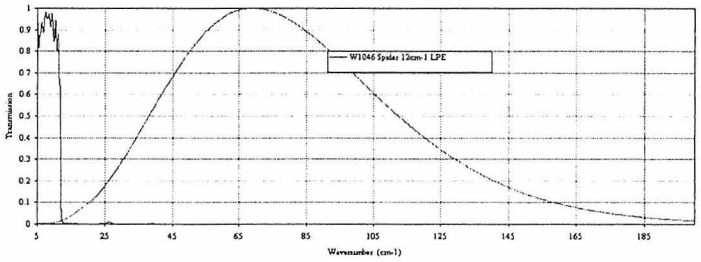

Figure 3.5: The LPE filter transmission spectra plotted with the normalized 20K blackbody curve

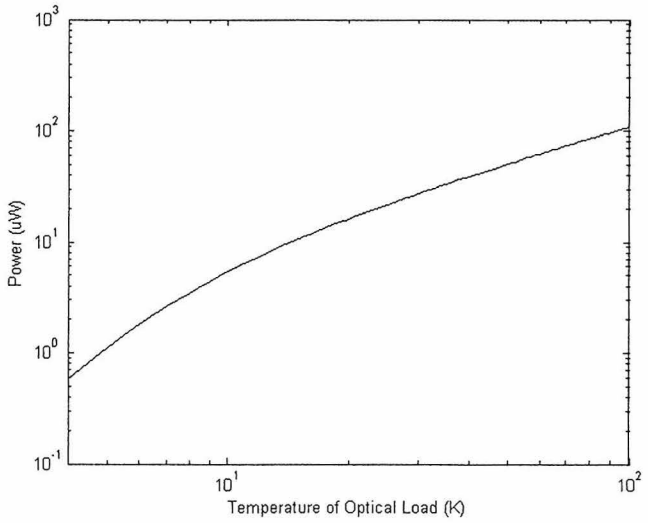

Figure 3.6: The power transmission that is expected through the LPE filter as a function of temperature of optical load

application because it is conductive at 4K, but its thermal conductivity reduces at higher temperatures, so it aids in reducing the boil off rate of the liquid helium when the warm load is being used. The load was blackened so that the radiation seen by the sapphire was of uniform temperature. A sketch of the configuration can be seen in figure 3.7.

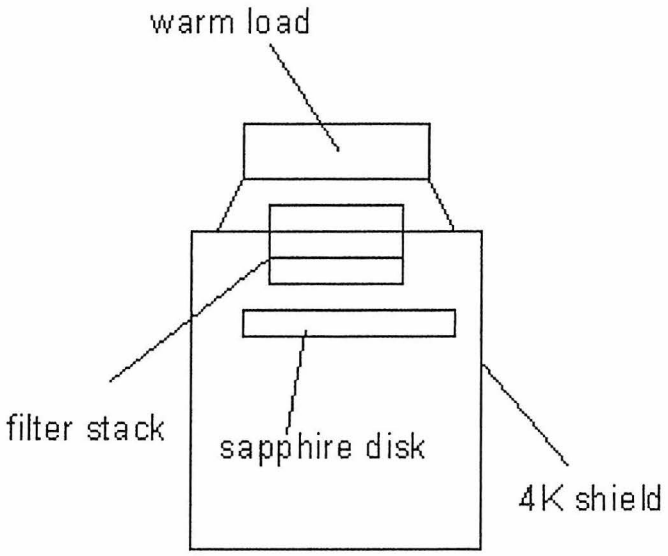

Figure 3.7: Sketch of the warm load and filter configuration for the optical tests

3.3 Theoretical Predictions of Practical Experimental Constraints

Testing the radiative properties of the blackened aluminum disk and the sapphire disks, though straightforward in theory, is not a trivial task. Because the cooling power from radiative cooling is so small at low temperature, the time constant for the samples to come to equilibrium at very low temperatures is quite long. Figure 3.8 shows the model for radiative cooling for the blackened aluminum baseline test which demonstrates the feasibility of completing these tests in a reasonable number of days, but also illustrates that length of time it takes to reach equilibrium will be a constrain on how quickly these various tests can be completed.

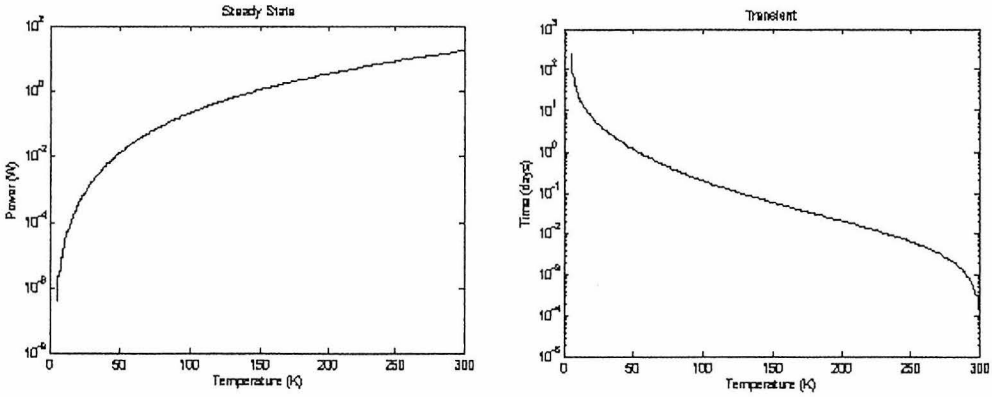

Figure 3.8: Transient and steady state prediction for aluminum temperature

Chapter 4

Results

4.1 Run 1

The point of this run was largely to test the cryogenics and thermometry. The data gathered from the first run was mostly qualitative. Another goal of this run was to cool the disk to around 4K and get a power versus temperature curve. This would then be used to precisely characterize the conductivity from the Kevlar and wires by fitting a power law to the data. We were not able to do this, however, because of the long time constant of the cool down. It was decided that since the cool down was taking so long it was clear that the wires and thread were not conducting significantly, so it was decided to end this run and change the arrangement.

4.2 Run 2

For this run the sample was cooled to 4K over a period of days. When the sample was cool calculated amounts of power were applied to the disk. Measurements of that power and the temperature that the disk equilibrated to were recorded. An exponential fit was done to the temperature versus time curves to find the equilibrium temperature. Then the power applied was plotted versus equilibrium temperature as shown in 4.1. The values can be found in table 1. The theoretical temperature was calculated using the formula

$$Power = \epsilon\sigma A(T_{hot}^4 - T_{cold}^4) \tag{4.1}$$

where ϵ is the emissivity, $\sigma = 5.67 \cdot 10^{-8}$ W/(m$^2\cdot$ K) T_{cold} is 4.6 (K) and A is the surface area of the sample.

These results are surprising because the experimental values do not match the theoretical values. For some reason the disk is able to dissipate more power for a given temperature than expected. It would be understandable that the disk might be less efficient at cooling than expected if the emissivity of the black paint was actually slightly less than one, but this result is harder to explain.

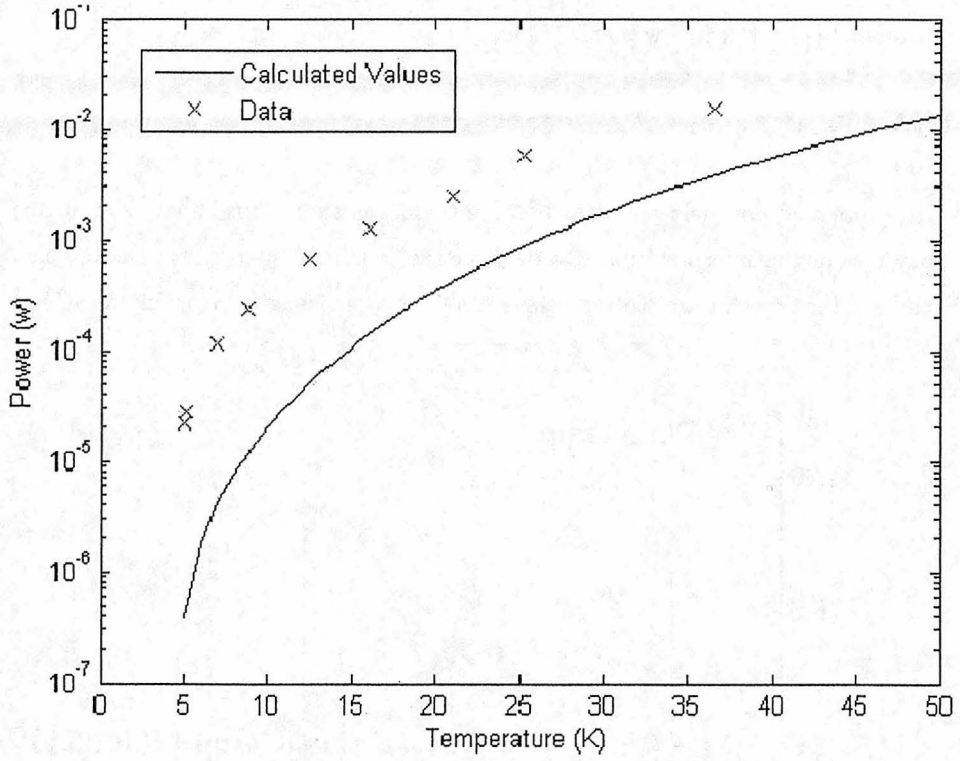

Figure 4.1: Run 2 Power versus Temperature Plot

It is likely that the heat switch contributed significantly to the cooling power and caused the disk to cool more efficiently, but there might also be some other explanation. The reason for thinking that there is some other explanation is that the data still appears to follow the curve of a T^4 power law that is off by a constant offset. This initially suggested a miscalculation that would make the theoretical value off by a constant factor, but no miscalculation was found. Gas cooling might also account for some of the cooling power. The temperature dependence for gas cooling is $T^{1/2}$. The discrepancy in the calculated and experimental value may be accounted for by some combination for these factors, but so far a successful fit to these parameters has not been achieved. Because it seemed that the heat switch was complicating the measurement, run 2 was ended and another run without the heat switch was conducted.

4.3 Run 3

Run three did not yield any data because there was anomalous behavior occurring that prevented any meaningful interpretation. To discover the source of the problem the temperatures of various parts of the cryostat are plotted versus time. This can be seen below in 4.2

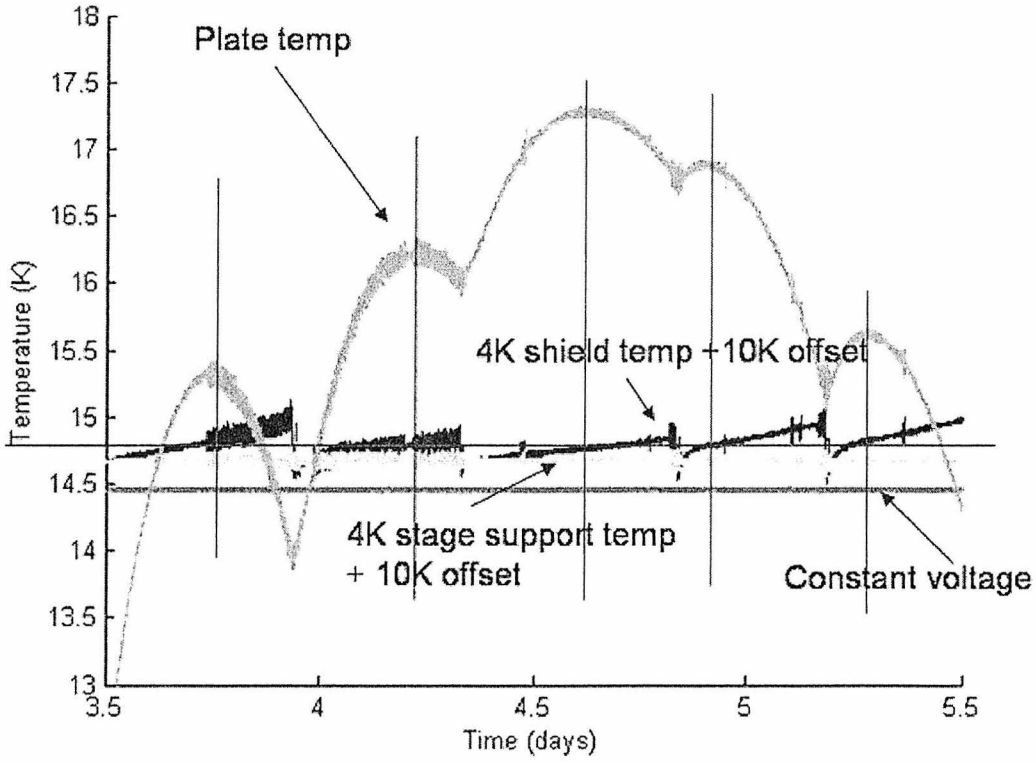

Figure 4.2: The temperature behavior versus time during run 3

The cyan line is the sample temperature. The blue line is the 4K shield temp +10K offset. The yellow line is the 4K stage support temp + 10K offset. The green line is a constant voltage in arbitrary units applied to the plate. It was postulated that the reason for the fluctuation in the plate temperature was that when the shield warmed up due to depletion of helium 4 in the tank, the carbon/Stycast mixture stopped cryogenically pumping and released gas into the vacuum space which then cooled the plate through gas conduction. Then when the helium 4 was refilled the shield cooled back down and the gas was pumped out of the vacuum space onto the walls. The red lines on the plot above show that the maxima of the sample temperature curves coincide with the moment where the shield temperature reaches a certain temperature. This theory was confirmed when it was discovered that the sharp drop in shield temperature shown in the graph above was correlated with the helium 4 transfers. It was also discovered that the reason for extra gas in the Dewar was a leak at the O-ring.

4.4 Run 4

This run was done with the cryostat and sample in the same configuration as in run 3, but with the O-ring leak fixed. Because of time constraints, this run was ended early, but the cryostat was left in the same configuration and run again shortly.

4.5 Run 5

The experimental procedure in run 5 was almost identical to that of run 2. Different amounts of power were applied to the disk and the equilibrium temperature was recorded. The data and the theoretical temperature for a given power are plotted in figure4.3. The theoretical temperature was calculated using the formula

$$Power = \epsilon\sigma A(T_{hot}^4 - T_{cold}^4) \tag{4.2}$$

where ϵ is the emissivity, $\sigma = 5.67 \cdot 10^{-8}$ W/(m^2 $\cdot$ K) T_{cold} is 4.6 (K) and A is the surface area of the sample.

4.6 Run 6

The experimental procedure for this run was also almost identical to that of run 5, except the sapphire disk was used. Different amounts of power were applied to the disk and the equilibrium temperature was recorded. Then the power versus temperature was plotted on the same plot with the data from run 5 as shown in figure 4.4.

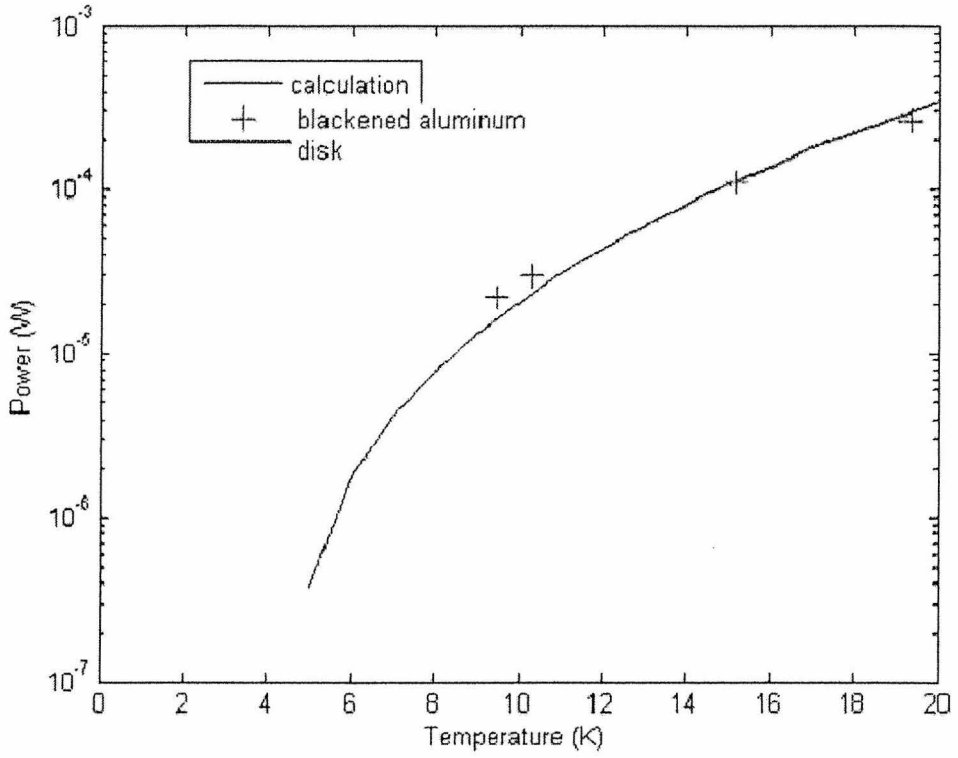

Figure 4.3: The total power dissipated versus temperature is plotted for the blackened aluminum disk

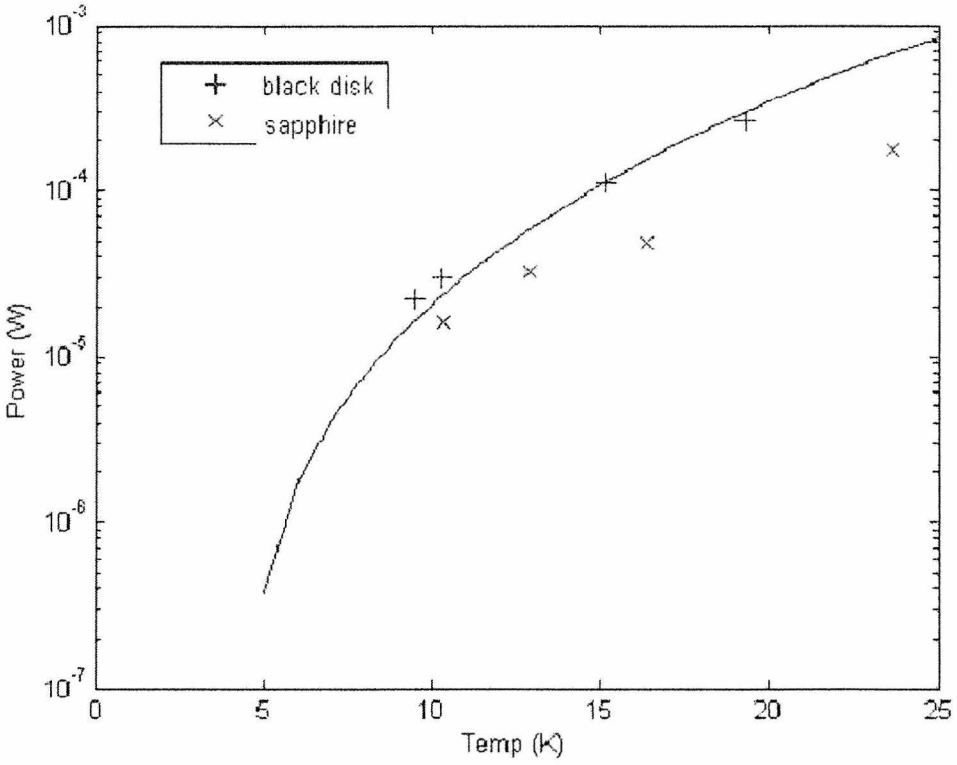

Figure 4.4: The total power (including lead, diode and radiative power) versus temperature is plotted for the blackened aluminum dis k as well as the sapphire

Equilibrium Temperature of Disk (K)	Theoretical Radiative Power for a Blackbody (W)	Actual Power Applied Including Diode Power (W)	Power Difference(W)	Lower Limit on Lead Conductance (w)	Lead area/length
9.4	1.58E-05	2.24E-05	-6.58E-06	14.88	-4.42E-07
10.2	2.23E-05	2.95E-05	-7.14E-06	17.36	-4.11E-07
15	1.08E-04	0.00011	-2.22E-06	53.24	-4.17E-08
19	2.79E-04	0.000265	1.46E-05	82.44	1.77E-07

Table 4.1: A lower limit on lead conductance.

4.7 Run 7

For run 7 the experimental procedure was different from the procedure used in the previous tests. Since optical testing was the goal of this experiment, the temperature of the warm load was varied and no power was applied to the disk. The temperature of the sapphire was recorded for each warm load temperature. The analysis of this data is more complicated for a variety of reasons. One of the more straight forward issues that must be addressed in this analysis is that the aperture for the filtered radiation is smaller than it will be in the actual implementation of the wave plate. The power that comes through the filters must be increased by a factor to compensate for this. The other analysis issue is that at most of the data points recorded in this run, the conductivity of the leads dominates the radiative cooling. We can get an accurate number for the warm load is at 66K, but to get something useful from the other data points, the data must be analyzed using information from the previous runs. For each of the last three runs (5,6,7) we can obtain some of the quantities in the equation

$$G_{lead}(T_s - T_b) + A(T_s - T_b) = Q_{rad} + Q_{htr} + Q_{diode} \tag{4.3}$$

and therefore solve for some of the unknown quantities using the system of three equations for the run.

One strategy for analyzing the data is to start with the data from run 5 that gives the equilibrium temperature the blackened aluminum disk reaches for a given power applied we can approximate the lead conduction. However, this assumes the blackened aluminum is a perfect blackbody, which is untested, so this provides a significant uncertainty in value for the lead conduction. If the data in figure 4.3 are used to calculate the lead uncertainly assuming that the blackened aluminum is a perfect blackbody, we can say that this is a lower limit on the lead conductance. This lower limit can be seen in table 4.1.

The power difference should be the power dissipation from the leads at a given temperature that is off by some error that is dependent on how close the blackened aluminum disk is to a blackbody. Since the radiative cooling is a significant factor at higher temperatures, we can justify using the lowest temperature to determine lead conductance. The last column in table 4.1 gives the area over

lower limit on lead conductance (W)	upper limit on lead conductance	power applied + diode power - lower limit on lead conductance (W)	power applied + diode power - upper limit on lead conductance (W)	actual temperature (K)
0.00000788	0.000016	8.12E-06	0	10.35
0.0000114	0.0000284	0.0000206	3.6E-6	12.95
0.000028	0.0000499	0.0000199	-2E-6	16.4
0.0000514	0.0001068	0.00012702	7.1E-5	23.65

Table 4.2: Lead conductance and total power - lead conductance at various temperature

Temperature of Warm Load (K)	Temperature of Disk (K)
6.6K +/- 0.1K	6.1K +/- 0.3K
10.3K +/- 0.5K	6.1 +/- 0.1K
30.1K +/- 0.2K	6.75K +/- 0.1K
66K +/- 1K	8.3K +/- 0.5K

Table 4.3: Sapphire temperature of a given warm load temperature

length factor for the leads. We can then use this to adjust the conductance of the leads at a given temperature by the A/L factor.

With this information about the conductivity of the leads we should be able to determine an upper limit on the amount of power for a given temperature that the sapphire is able to radiate using the data in run 6. We look at the results for run 6 that are shown in figure 4.4. Since the lead conductance is uncertain, we can say that for the lowest temperature point the contribution is anywhere from the lower limit calculated using the data in table 4.1 to the entirety of the power measured at that temperature. This means that the lead conductance is between $7.88 \cdot 10^{-6}$W and $16 \cdot 10^{-6}$. We can use these values to get an upper limit on the lead conductance for higher termeratures. This is done by taking the upper limit on the lead conductance and dividing by the thermal conductivity at 10.35K. This give the A/L factor which can be multiplied by the thermal conductivity at the higher temperatures to get the lead conductance. The plot of this result is shown in figure 4.5.

The data from the seventh run can be seen in table 4.3. This table shows the temperature of the sapphire for each warm load temperature.

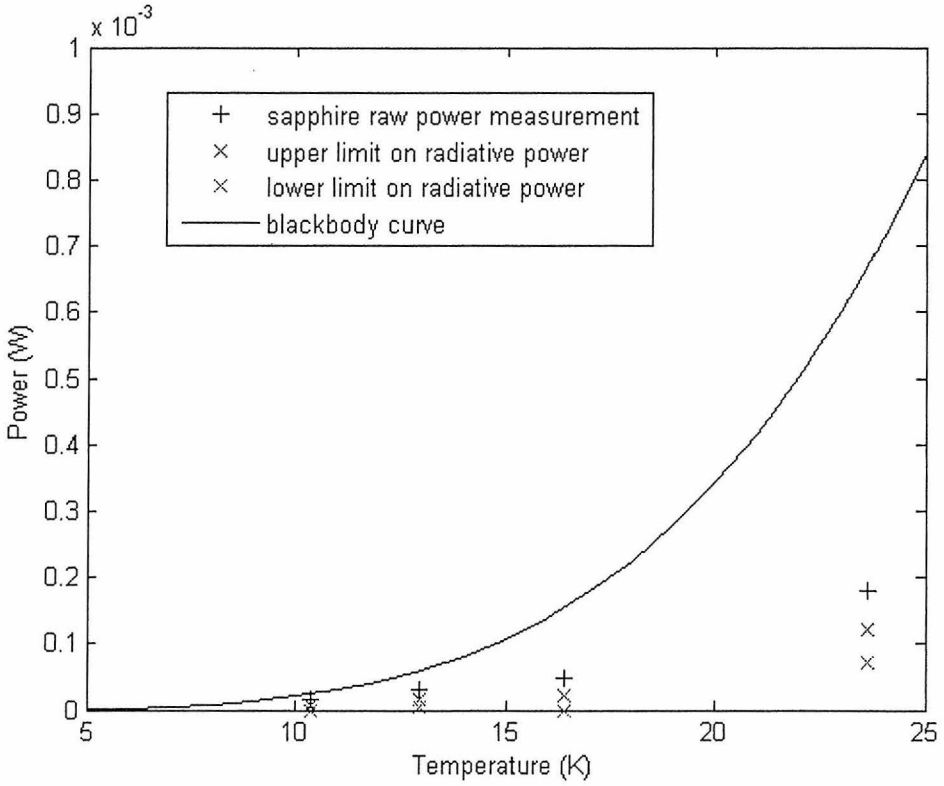

Figure 4.5: This plot shows the upper and lower limit on radiative power of the sapphire

Chapter 5

Discussion and Future Work

The information gathered during this project has given us some understanding of the behavior of sapphire at cryogenic temperatures. We can see that compared to the radiative cooling power of the sapphire, conduction through the leads is dominant at these temperatures. One consequence of this discovery is that we see that physical contact of any kind (such as gas cooling) will be vastly more efficient and effective than radiative cooling from the sapphire itself.

This result also leads to the conclusion that we should utilize the flange that will be holding the sapphire wave plate. To do this we would design a flange that is blackened such that its emissivity is ~ 1 and is of the appropriate area to provide cooling power needed. This is feasible because the high thermal conductivity of sapphire at 4K (greater than that of copper) will allow the wave plate temperature to equilibrate quickly with the flange. The filter transmission spectra can be used to determine how much power from the 20K blackbody will go through the filters and hit the wave plate. This calculation can be found in the section on filters. This is an upper limit on the power because this assumes all the radiation transmitted through the filters is absorbed by the wave plate. Then the equation

$$Power = \epsilon\sigma A(T_{bath}^4 - T_{waveplate}^4) \tag{5.1}$$

where ϵ is the emissivity, $\sigma = 5.67 \cdot 10^{-8}$ W/($m^2 \cdot$ K) and A is the surface area, can be used. Knowing the power, we can solve for the area A of the flange required for given wave plate and bath temperatures. The area needed in the scenario where the bath is at 20K and the optical load is 60K can be seen in figure 5.1. The scenario where the bath is at 4K and the optical load is 20K can be seen in figure 5.2.

These plots show that for both and optimistic and pessimistic scenario a reasonably sized flange can be used to provide cooling power to the wave plate. The sapphire wave plate is intended to be 30.5cm in diameter and 3mm think so the surface area of the side of the wave plate alone is

thick

$$\pi dh = \pi 30.5cmx0.3cm = 28.7cm^2 \tag{5.2}$$

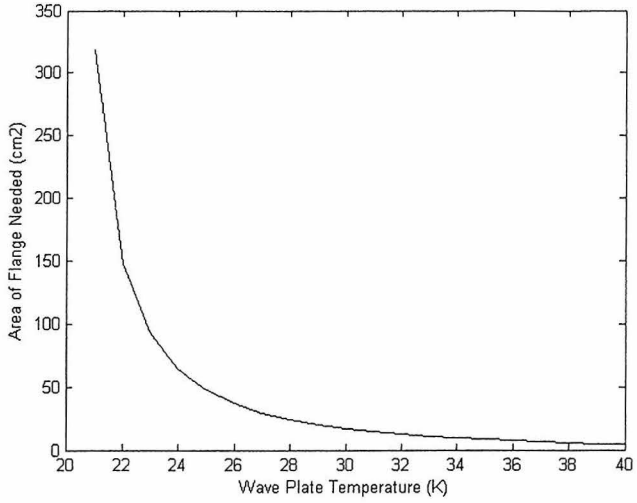

Figure 5.1: Flange area versus equilibrium wave plate temperature for an optical load of 60K and a bath temperature of 20K. Under these conditions we will get the wave plate to temperature of approximately 27K with just the side of the wave plate blackened.

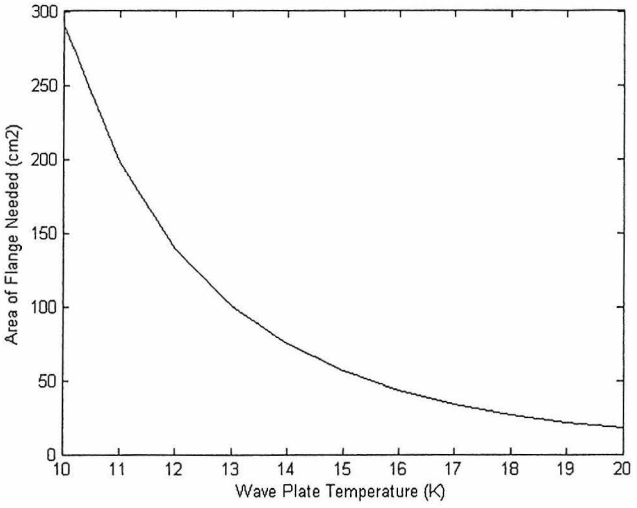

Figure 5.2: The flange area versus equilibrium wave plate temperature for an optical load temperature of 20K and a bath temperature of 4K. Under these conditions we will get to a wave plate temperature of about 19K with just the side of the wave plate blackened.

We can see on the plots in 5.2 and 5.1 and equation 5.2 that blackening only the side of the wave plate would provide the cooling power to keep the wave plate at less than 27K in the pessimistic situation. 27K is a temperature which contributes negligibly to the total background loading because as can be seen in 4.5 the upper limit for emissivity of the sapphire is about 10-20%, so the excess loading will be a few Kelvin.

Another consequence of the discovery of the dominance of parasitic cooling is that it clear one of the next steps in this investigation should be to run tests where parasitic loading is eliminated The uncertainty of conduction through wiring and supports should be eliminated by moving on to testing in a situation that is similar to the situation the wave plate will eventually be in. It would be possible to carry these next tests out using the low temperature apparatus with a superconducting bearing that is currently being built at Case Western [10]. Because it would be levitated there would be no conductive cooling through supports. A bolometer could be used to measure the temperature so that diode thermometers are not necessary. It would be very useful to characterize the exact thermal behavior of the wave plate in a situation that mimics the situation in flight, so that any significant effects can be remedied or addressed when analyzing the data.

Bibliography

[1] http://www.astro.ubc.ca/people/scott/cmb_intro.html.

[2] T. Miyashita and A. Crites. A radiotelescope for observations of astrophysical polarized radiation. SURF report, October 2003.

[3] http://www.astro.caltech.edu/~lgg/spider_front.htm.

[4] P. de Bernardis et al. *Nature*, 404:955–2000, 2000.

[5] http://astro.uchicago.edu/dasi/DASIPOL-science.pdf.

[6] B. Philhour. PhD dissertation, Caltech, 2002.

[7] A.C.S. Readhead. *Science*, 306:836–844, 2004.

[8] J.M. Kovac E.M. Leitch C. Pryke J.E. Carlstrom N.W. Halverson and W.L. Hozapfel. *Nature*, 420:772–787, 2002.

[9] T.E. Montroy et al. A measurement of the cmb ¡ee¿ spectrum from the 2003 flight of boomerang. submitted to ApJ, 2005. astro-ph/0507514, 2005.

[10] T.E. Montroy et al. Spider: A new balloon-borne experiment to measure cmb polarization on large angular scales. Proceedings of the SPIE., April 2006.

[11] Bock, J. June 20, 2005. Personal Correspondence.

[12] http://www.lakeshore.com/temp/acc/am_wirepo.html.

[13] Tucker, Carole. April 28, 2006. Correspondence.